

Pressure instability of bcc iron

Hong Ma and S. L. Qiu

Department of Physics, Alloy Research Center, Florida Atlantic University, Boca Raton, Florida 33431-0991

P. M. Marcus

IBM Research Division, T. J. Watson Research Center, Yorktown Heights, New York 10598

(Received 23 October 2001; revised manuscript received 24 January 2002; published 17 July 2002)

First-principles total-energy calculations with WIEN97 on ferromagnetic iron in body-centered tetragonal structure under hydrostatic pressure have shown that the body-centered cubic (bcc) phase exists up to 1500 kbar of pressure. At that pressure a shear constant vanishes and the phase becomes unstable. A body-centered tetragonal (bct) phase is shown to come into existence at 1300 kbar and becomes stable at 1825 kbar and above. The minima of a free energy evaluated along the epitaxial Bain path generalized to finite pressure give the tetragonal phases of iron under pressure. Second derivatives of the free energy at the minima define elastic constants of both the bcc and bct phases as functions of pressure, which are appropriate to determine stability. These elastic constants are the same functions of pressure as the usual elastic constants computed from stress-strain relations under pressure. Minima of tetragonal energies calculated at constant volume are shown to be unreliable for determining stability of a phase.

DOI: 10.1103/PhysRevB.66.024113

PACS number(s): 75.10.Lp, 75.50.Bb, 62.20.Dc, 61.50.Ks

I. INTRODUCTION

Under hydrostatic pressure the ferromagnetic (FM) bcc ground state of Fe has decreased magnetization and decreased stability. At the stability-limit pressure p_s this phase of Fe becomes unstable. In previous work, the value of p_s has been estimated¹ as 1000 kbar and as² above 2000 kbar. This work fixes the value of p_s at 1500 kbar by evaluating as a function of pressure p the shear constant $C' \equiv (c_{11} - c_{12})/2$ that goes to zero at p_s .

The procedure used to evaluate $C'(p)$ treats FM Fe in body-centered tetragonal (bct) structure at a given p and shows that there is a bcc equilibrium structure at pressures up to p_s . The equilibrium state at each p is found from the epitaxial Bain path (EBP) of FM Fe, which was previously used to find the equilibrium states at $p=0$ of tetragonal Fe in various magnetic phases.³ For this work the EBP, which is a special path through tetragonal states that goes through all the equilibrium states, has been generalized to finite p .

The calculation of the EBP finds the total energy E in each tetragonal state on the path. At $p=0$ the equilibrium states of the magnetic phases of Fe are given by the minima of E . However, at finite p the phases are found from the minima of a free energy (at zero temperature) $G \equiv E + pV$ evaluated along the EBP, where E is the energy per atom and V is the volume per atom. The elastic constants C' and c_{44} at each p are defined as second derivatives of G at the minima of G taken with respect to particular shear strains. The pressure dependences of C' and c_{44} are shown to be the same as the pressure dependences calculated from stress-strain relations under pressure.

The calculations of G for increasing p show that before the pressure reaches p_s , where the bcc minimum of G vanishes, a new noncubic tetragonal minimum of G forms, which persists for $p > p_s$ and becomes stable at $p \geq 1825$ kbar.

The paper is organized as follows. Section II describes the

calculation procedures and shows why the minima of G along the EBP give the equilibrium states at finite p . Section III gives the results of the calculations of G and the elastic constants of the bcc and bct states at p values up to 2000 kbar. Section IV discusses the pressure dependence of elastic constants, why constant volume calculations fail to determine stability, the relation of fcc Fe to bcc Fe, and the status of the bct phase.

II. PROCEDURES

At each point on the tetragonal plane (coordinates a and c or, equivalently, c/a and $V = ca^2/2$ per atom), the total energy of the body-centered tetragonal lattice $E(a, c)$ can be calculated from first principles. In addition to the energy, the stresses in the basal plane

$$\sigma_1 = \sigma_2 = \frac{1}{ac} \left(\frac{\partial E(a, c)}{\partial a} \right)_c \quad (1)$$

and out of the basal plane

$$\sigma_3 = \frac{2}{a^2} \left(\frac{\partial E}{\partial c} \right)_a \quad (2)$$

can be calculated.

The path on the tetragonal plane called the EBP is found at $p=0$ for each a by using Eq. (2) and the condition $\sigma_3 = 0$. Along the EBP the functions $E^{\text{EBP}}(a)$ and $V^{\text{EBP}}(a)$ are then known, and by construction $[\partial E(a, c)/\partial c]_a = 0$ at every point of the EBP. Then at a minimum of $E^{\text{EBP}}(a)$, coordinates a_0, c_0 , the derivative of $E(a, c)$ vanishes along the EBP and also along c . Thus the two components of the gradient of $E(a, c)$ on the tetragonal plane must both vanish and a_0, c_0 give a tetragonal energy minimum and corresponds to an equilibrium state in which the stresses given by Eqs. (1) and (2) vanish.⁴

To generalize the EBP to finite p requires two changes in the procedure used at $p=0$. The first change is to use Eq. (2) to find the c at each a at which $\sigma_3 = -p$. This procedure finds the EBP at p and the functions $E^{\text{EBP}}(a;p)$ and $V^{\text{EBP}}(a;p)$. The notation indicates that p is a given parameter, and E^{EBP} and V^{EBP} are functions of a (or c/a) alone at that p .

The second change is to define a free energy at that p (and at zero temperature), which is also the enthalpy at zero temperature,

$$G(a,c;p) \equiv E(a,c) + pV(a,c), \quad (3)$$

and look for minima, coordinates a_0, c_0 , of

$$G^{\text{EBP}}(a;p) \equiv E^{\text{EBP}}(a;p) + pV^{\text{EBP}}(a;p). \quad (4)$$

At a_0, c_0 using Eq. (2) and $p = -\sigma_3$

$$\begin{aligned} \left(\frac{\partial G(a,c;p)}{\partial c} \right)_{a_0,c_0} &= \left(\frac{\partial E(a,c)}{\partial c} \right)_{a_0,c_0} + p \left(\frac{\partial V(a,c)}{\partial c} \right)_{a_0,c_0} \\ &= \sigma_3(a_0,c_0) \frac{a_0^2}{2} - \sigma_3(a_0,c_0) \frac{a_0^2}{2} = 0. \end{aligned} \quad (5)$$

Since the derivative of $G(a,c;p)$ at a_0, c_0 also vanishes along the EBP, a_0, c_0 give a tetragonal minimum of $G(a,c;p)$ by the same argument used for $p=0$, and

$$\left(\frac{\partial G(a,c;p)}{\partial a} \right)_{a_0,c_0} = \left(\frac{\partial G(a,c;p)}{\partial c} \right)_{a_0,c_0} = 0. \quad (6)$$

Furthermore at a_0, c_0 the in-plane stresses σ_1 and σ_2 are given by, using Eqs. (1), (3), and (6),

$$\begin{aligned} \sigma_1 = \sigma_2 &= \frac{1}{a_0 c_0} \left(\frac{\partial E(a,c)}{\partial a} \right)_{a_0,c_0} = \frac{1}{a_0 c_0} \left(\frac{\partial G(a,c;p)}{\partial a} \right)_{a_0,c_0} \\ &\quad - \frac{p}{a_0 c_0} \left(\frac{\partial V(a,c)}{\partial a} \right)_{a_0,c_0} = 0 - p = -p. \end{aligned} \quad (7)$$

Thus at a_0, c_0 the system is under hydrostatic pressure p , and $G(a_0,c_0;p)$ is a tetragonal minimum of $G(a,c;p)$ and an equilibrium state under pressure p , i.e., no other stresses than hydrostatic p are required to maintain the state. This equilibrium state will be stable if G increases for all small strains, not just strains that preserve tetragonal symmetry. The stability can be tested by well-known algebraic conditions on elastic constants (see, for example, Ref. 5, p. 142) defined by

$$c_{ij} = \frac{1}{V} \left(\frac{\partial^2 G(a,c;p)}{\partial \varepsilon_i \partial \varepsilon_j} \right)_{a_0,c_0}, \quad i, j = 1 \text{ to } 6. \quad (8)$$

Then the variation of G around the extremum a_0, c_0 for small strains is a quadratic function of the strains given by

$$\delta^2 G = \frac{V}{2} \sum_{i,j=1}^6 c_{ij} \varepsilon_i \varepsilon_j. \quad (9)$$

The stability conditions on the c_{ij} express the positive definiteness of Eq. (9) for all strains, and will be given explicitly for tetragonal and cubic symmetry below. The pressure at which bcc Fe becomes unstable will be the pressure at which Eq. (9) fails to be positive definite.

The elastic constants defined by Eq. (8) differ from elastic constants defined by the corresponding derivatives of $E(a,c)$ at a_0, c_0 by the contribution of the pV term in Eq. (3). Let \bar{c}_{ij} be the elastic constants from E defined by

$$\bar{c}_{ij} = \frac{1}{V} \left(\frac{\partial^2 E(a,c)}{\partial \varepsilon_i \partial \varepsilon_j} \right)_{a_0,c_0}. \quad (10)$$

The \bar{c}_{ij} are the usual elastic constants at $p=0$ and a_0, c_0 give the equilibrium state at $p=0$, but at finite p the point a_0, c_0 is not at a minimum of $E(a,c)$. Then

$$c_{11} = \frac{2}{c_0} \left(\frac{\partial^2 G(a_1, a_2, c; p)}{\partial a_1^2} \right)_{a_0, c_0} = \bar{c}_{11} + \frac{2}{c_0} \frac{\partial^2 (pV)}{\partial a_1^2} = \bar{c}_{11}, \quad (11)$$

where $V = a_1 a_2 c / 2$ and only one side of the tetragonal base is strained. Similarly

$$c_{11} + c_{12} = \frac{1}{c_0} \left(\frac{\partial^2 G(a,c;p)}{\partial a^2} \right)_{a_0, c_0} = \bar{c}_{11} + \bar{c}_{12} + p, \quad (12)$$

$$c_{33} = \frac{2c_0}{a_0^2} \left(\frac{\partial^2 G(a,c;p)}{\partial c^2} \right)_{a_0, c_0} = \bar{c}_{33}, \quad (13)$$

$$c_{66} = \frac{2}{c_0 a_0^2} \left(\frac{\partial^2 G(a,c, \theta_{12}; p)}{\partial \theta_{12}^2} \right)_{a_0, c_0, \pi/2} = \bar{c}_{66} - \frac{p}{2}, \quad (14)$$

where to second order in $\delta\theta_{12}$ $V = (ca^2/2)(1 - \delta\theta_{12}^2/4)$; similarly

$$\begin{aligned} c_{44} = c_{55} &= \frac{2}{c_0 a_0^2} \left(\frac{\partial^2 G(a,c, \theta_{23}; p)}{\partial \theta_{23}^2} \right)_{a_0, c_0, \pi/2} \\ &= \bar{c}_{44} - \frac{p}{2} = \bar{c}_{55} - \frac{p}{2}. \end{aligned} \quad (15)$$

Then $c_{13} = \bar{c}_{13} + p$ can be found from the curvature of the EBP at a_0

$$Y' = \frac{1}{c_0} \left(\frac{d^2 G^{\text{EBP}}(a;p)}{da^2} \right)_{a_0} = c_{11} + c_{12} - \frac{2c_{13}^2}{c_{33}}. \quad (16)$$

For a cubic structure, $c_{33} = c_{11}$, $c_{13} = c_{12}$, and

$$Y' = \frac{(c_{11} + 2c_{12})(c_{11} - c_{12})}{2c_{11}}. \quad (17)$$

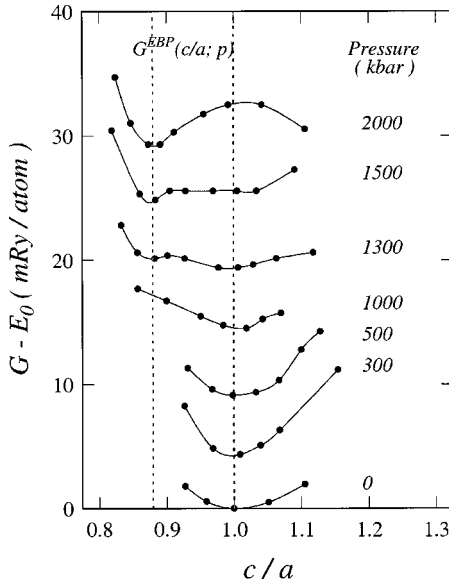


FIG. 1. $G^{\text{EBP}}(c/a;p)$ curves in the vicinity of the bcc point ($c/a=1$) at pressures of 0, 300, 500, 1000, 1300, 1500, and 2000 kbar. E_0 is the energy per atom in the bcc FM ground state at zero pressure. For clarity, the $G^{\text{EBP}}(c/a;p)$ curves at pressures from 300 to 2000 kbar are shifted toward E_0 by 145, 233, 441, 555, 625, and 798 mRy/atom, respectively. The solid lines interpolate between the calculated points.

Hence both $C' \equiv (c_{11} - c_{12})/2$ and Y' vanish together for a cubic structure.

The EBP's of FM tetragonal Fe as a function of pressure were found by first-principles total-energy calculations using the full-potential linearized-augmented-plane-wave (FLAPW) method with the Perdew-Burke-Ernzerhof exchange-correlation potential in a generalized-gradient approximation (GGA).⁶ A plane-wave cutoff $R_{\text{MT}}K_{\text{max}}=9$, $G_{\text{max}}=14$ and 300 k points in the irreducible wedge of the Brillouin zone were used in all the calculations reported here. We found that, although it takes much longer computing time, it is necessary to use $R_{\text{MT}}=1.5$ a.u. in order to get rid of the ghost bands in the $G^{\text{EBP}}(a;p)$ calculations at finite pressure. The k -space integration was done by the modified tetrahedron method.⁶ A two-atom tetragonal unit cell with parallel spins was used. All the calculations were highly converged. Tests with larger basis sets and different Brillouin-zone samplings yielded only very small changes in the results. The convergence criterion on the energies is set at 5×10^{-3} mRy per atom.

III. RESULTS

Figure 1 shows the $G^{\text{EBP}}(c/a;p)$ curves of FM tetragonal Fe in the vicinity of the bcc point ($c/a=1$) at pressures from zero to 2000 kbar, where the reference energy E_0 is the energy per atom in the bcc FM ground state at zero pressure. For clarity, the $G^{\text{EBP}}(c/a;p)$ curves at pressures from 300 to 2000 kbar are shifted toward E_0 by 145, 233, 441, 555, 625, and 798 mRy/atom, respectively. The $G^{\text{EBP}}(c/a;p)$ curve has a minimum at the bcc point at pressures less than 1500 kbar, becomes flat at ~ 1500 kbar and then has a negative

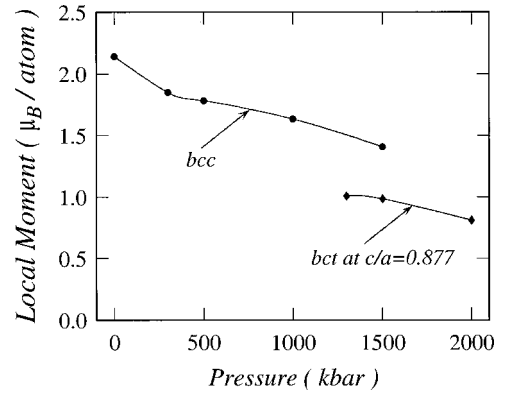


FIG. 2. The local magnetic moments of FM Fe in the bcc and bct phases as functions of pressure. The solid lines interpolate between the calculated points.

curvature at pressures above 1500 kbar, indicating that the bcc state is unstable at $p \geq 1500$ kbar.

Figure 1 also shows that a new bct state at $c/a=0.877$ develops starting from $p=1300$ kbar at which the $G^{\text{EBP}}(c/a;p)$ curve has a minimum in addition to the bcc state. With increasing pressure the minimum becomes deeper corresponding to a larger positive curvature. Similar to the bcc state the bct state is also ferromagnetic. Figure 2 shows the local moments of both the bcc and bct states as functions of pressure.

To study the stability of both the bcc and the bct phases of FM Fe we have calculated the elastic constants of each phase using Eqs. (11)–(16). Figures 3(a) and 3(b) show the elastic constants c_{11} , c_{12} , c_{44} , the shear constant C' and the modified Young's modulus Y' of the bcc phase as functions of pressure. Since the system is at zero temperature, stability here means mechanical stability. For a cubic crystal the stability conditions⁵ can be given in terms of the three elastic constants; they express the positive definiteness of the strain energy with respect to all small deformations of the lattice. These conditions are

$$c_{11} > |c_{12}|, \quad c_{11} + 2c_{12} > 0, \quad c_{44} > 0. \quad (18)$$

Figure 3(a) shows that the bcc state is stable at $p < 1500$ kbar since all three conditions in Eq. (18) are satisfied. Figure 3(b) shows that both C' and Y' vanish at $p = 1500$ kbar, which is then the precise value of the stability-limit pressure p_s . At $p > p_s$ both C' and Y' become negative, which indicates that the bcc state has become unstable due to the violation of the first stability condition in Eq. (18).

The elastic constants c_{11} , c_{12} , c_{13} , c_{33} , c_{44} , c_{66} , and the shear constant C' of the bct phase as functions of pressure are shown in Fig. 4. The stability conditions for a tetragonal crystal⁵ are

$$c_{11} > |c_{12}|, \quad (c_{11} + c_{12})c_{33} > 2c_{13}^2, \quad c_{44} > 0, \quad c_{66} > 0. \quad (19)$$

The first stability condition in Eq. (19) is equivalent to $C' > 0$, which is violated at $p < 1825$ kbar as shown in Fig. 4, indicating that the bct state is unstable at pressures less than 1825 kbar. Comparison of Eq. (19) with Eq. (16) reveals that

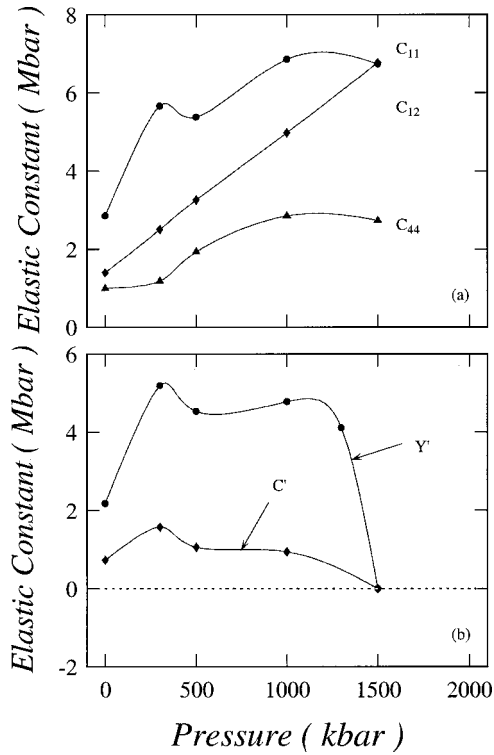


FIG. 3. (a) The elastic constants c_{11} , c_{12} , c_{44} of the bcc state of FM Fe as a function of pressure. (b) The shear constant C' and the modified Young's modulus Y' of the bcc phase of FM Fe as a function of pressure. Both C' and Y' vanish at $p=1500$ kbar, which is the precise value of the stability-limit pressure p_s . The solid lines interpolate between the calculated points.

the second stability condition in Eq. (19) is equivalent to $Y' > 0$. As mentioned above, the $G^{\text{EBP}}(c/a; p)$ curve of the bct state shown in Fig. 1 has a positive curvature corresponding to a positive Y' for $p > 1300$ kbar. Hence the second stability condition in Eq. (19) is always satisfied. The third and fourth conditions in Eq. (19) are also satisfied since c_{44} and c_{66} of the bct state are positive in the entire region of pressure shown in Fig. 4. The shear constant C' first be-

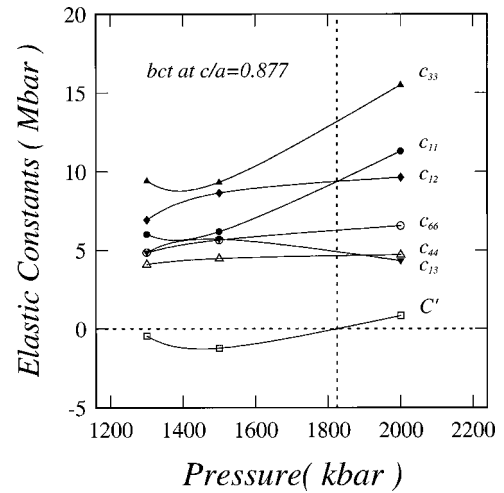


FIG. 4. The elastic constants c_{11} , c_{12} , c_{13} , c_{33} , c_{44} , c_{66} , and the shear constant C' of the bct phase of FM Fe at $c/a=0.877$ as a function of pressure. The change in sign of C' at $p=1825$ kbar indicates that the bct phase becomes stable at $p > 1825$ kbar. The solid lines interpolate between the calculated points.

comes positive at $p > 1825$ kbar, when all four of the conditions in Eq. (19) are satisfied and the bct state becomes stable at $p > 1825$ kbar.

For comparison of the present work with previous publications⁷⁻¹⁰ we tabulate in Table I the values of the elastic constants c_{11} , c_{12} , c_{44} , the shear constant C' , and the modified Young's modulus Y' of bcc FM Fe as functions of pressure. The calculated elastic constants of the bct phase are plotted in Fig. 4, but to our knowledge no elastic constants of the bct state have been reported.

IV. DISCUSSION

The elastic constants defined here by Eqs. (3) and (8) are second derivatives of the free energy $G(a, c; p)$ at equilibrium for each p . They are the quantities needed in the stability conditions (18) and (19) to prove that G is a minimum at

TABLE I. Elastic constants c_{11} , c_{12} , c_{44} , Y' , and C' of FM bcc Fe as a function of pressure.

	Pressure (kbar)	V_0 ($\text{\AA}^3/\text{atom}$)	c_{11} (Mbar)	c_{12} (Mbar)	c_{44} (Mbar)	C' (Mbar)	Y' (Mbar)
Present work	0	11.576	2.852	1.394	0.995	0.729	2.174
	300	10.357	5.656	2.507	1.182	1.575	5.190
	500	9.908	5.372	3.261	1.932	1.056	4.532
	1000	8.857	6.856	4.971	2.850	0.943	4.779
	1500	8.130	6.738	6.772	2.801	0	0
Ref. 7	0	11.40	2.79	1.40	0.99	0.69	
Ref. 8 ^a	0	11.78	2.431	1.381	1.219	0.525	
Ref. 9 ^a	10		2.62	1.55	1.28	0.54	
Ref. 10 ^a	46		2.81	1.44	1.23	0.69	

^aExperimental results.

equilibrium for all small strains, i.e., that the equilibrium state is stable. We compare the c_{ij} with the elastic constants c_{ij}^{BK} derived by Barron and Klein¹¹ from stress-strain relations under pressure and used, for example, by Karki *et al.*¹² to find instabilities. The comparison shows that all the c_{ij} have the same p dependences as the c_{ij}^{BK} ; thus from Eqs. (11)–(15) and Eqs. (5.7) and (B4) of Ref. 11 $c_{11}^{\text{BK}} = c_{11} = \bar{c}_{11}$, $c_{12}^{\text{BK}} = c_{12} = \bar{c}_{12} + p$, $c_{44}^{\text{BK}} = c_{44} = \bar{c}_{44} - p/2$.

By their construction the c_{ij} are appropriate elastic constants to determine phase stability. Our construction also gives the c_{ij} and the equilibrium value of G directly as functions of p . Hence a thermodynamic phase transition could be easily determined by the crossing pressure of two $G(p)$ (or enthalpy) curves. These curves could be for the bcc and hcp phases of Fe to fix the pressure of the bcc to hcp phase transition. The differences of the enthalpy curves of bcc and fcc Fe from hcp Fe as functions of p are plotted by Stixrude and Cohen,¹³ to show the bcc→hcp transition at about 100 kbar.

Stixrude *et al.*¹ estimated $p_s = 1000$ kbar from two $E(c/a)$ curves at constant volume—one at $V = 70$ a.u. corresponding to $p = 0$ shows a minimum at $c/a = 1$ and one at $V = 50$ a.u. corresponding to $p = 2000$ kbar shows a maximum at $c/a = 1$. Söderlind *et al.*² concluded that $p_s > 2000$ kbar because their $E_V(c/a)$ curve showed a shallow minimum at $c/a = 1$ at $V = 7.55 \text{ \AA}^3 = 50.9$ a.u. corresponding to 2000 kbar (their Fig. 6). Reference 1 missed the shallow minimum at 2000 kbar because the values of c/a used were not spaced closely enough. We have verified the shallow minimum at 2000 kbar. But our Fig. 1 shows clearly that $G^{\text{EBP}}(c/a; p)$ at $p = 2000$ kbar has a maximum at $c/a = 1$, indicating $Y' < 0$ and instability. Thus conclusions about stability from minima of $E_V(c/a)$ curves are not reliable.

Our value of 1500 kbar for the critical pressure of bcc Fe is also the value given in Ref. 13. Reference 13 uses the disappearance of the minimum at $c/a = 1$ in a tetragonal energy calculation at constant volume, the same procedure as was used in Refs. 1 and 2. However, Ref. 13, similar to Ref. 1, misses the minimum at 2000 kbar found in Ref. 2. Hence the correspondence of the estimate of critical pressure to ours is accidental.

In addition to the bcc phase at the minimum of $G^{\text{EBP}}(a; p)$ at $c/a = 1$, there is a second minimum at c/a near $\sqrt{2}$ in each magnetic phase. These phases of γ -Fe have been studied at $p = 0$.¹⁴ In particular a nonmagnetic (NM) phase has fcc structure with an energy substantially larger than the bcc phase. The free energy or enthalpy of the NM fcc phase

increases more slowly than the bcc phase with increasing pressure and the fcc phase becomes more stable than the bcc phase at some pressure. From Ref. 13 this phase transition could take place around 300 kbar. But the hcp phase, also NM, has still lower free energy and the transition from the bcc phase occurs at a lower pressure. The NM fcc Fe phase is best discussed along with the hcp phase and is not considered in this paper.

Brown *et al.*¹⁵ observed experimentally a sound velocity discontinuity in Fe at 2000 kbar and suggested that it was a solid-solid transition at the γ - ϵ phase boundary. Ross *et al.*¹⁴ suggested that the shock anomaly at 2000 kbar may be the transition to a new high-pressure solid α' phase with a bcc structure. Söderlind *et al.*² suggested that the α' phase corresponds to a bct state at $c/a = 0.875$ with substantial magnetic moment. However, Söderlind *et al.*² pointed out that they did not know whether this bct state is stable at high pressure. We have shown here from the free energy $G^{\text{EBP}}(c/a; p)$ and the elastic constants calculations that the bct state at $c/a = 0.877$ develops starting from $p = 1300$ kbar and becomes stable at $p > 1825$ kbar. Stable here could be called metastable because the hcp phase has a lower G (or enthalpy) value than the bct phase; stable also could be called mechanically stable since the calculations are at $T = 0$. But the fact that the bct phase becomes stable in just the region (from 2000 kbar) where the α' phase is observed supports the suggestion of Söderlind *et al.*² The α' phase cannot be the bcc phase because bcc Fe is unstable above 1500 kbar, which is well below the observation pressure of the α' phase.

There is still a considerable difference in the G values of the bct and hcp phases at $T = 0$, which could be called a thermodynamic instability of the bct phase. The sign of the difference must be reversed by the entropy term in G at high temperature if the bct phase is to become the ground state. Proof of such a reversal requires quantitative evaluation of entropies in each phase. However, some qualitative support comes from the low value of C' for the bct phase shown in Fig. 4, which could make the bct vibrational entropy unusually large.

ACKNOWLEDGMENTS

The calculations were carried out using the computational resources provided by the MDRCF, which is funded jointly by the NSF and FAU. Hong Ma wishes to thank the financial support from the Department of Physics at Florida Atlantic University. P. M. M. thanks IBM for providing facilities via the Thomas J. Watson Research Center.

¹L. Stixrude, R. E. Cohen, and D. J. Singh, Phys. Rev. B **50**, 6442 (1994).

²P. Söderlind, J. A. Moriarty, and J. M. Wills, Phys. Rev. B **53**, 14 063 (1996).

³S. L. Qiu, P. M. Marcus, and Hong Ma, Phys. Rev. B **64**, 104431 (2001).

⁴P. Alippi, P. M. Marcus, and M. Scheffler, Phys. Rev. Lett. **78**,

3892 (1997); P. M. Marcus and P. Alippi, Phys. Rev. B **57**, 1971 (1998).

⁵J. F. Nye, *Physical Properties of Crystals* (Clarendon Press, Oxford, 1985).

⁶Peter Blaha, Karlheinz Schwarz and Joachim Luitz, *User's Guide for WIEN97*, Vienna University of Technology, 1997; P. Blaha, K. Schwarz, and S. B. Trickey, Comput. Phys. Commun. **59**, 399

- (1990).
- ⁷G. Y. Guo and H. H. Wang, *Chin. J. Phys. (Taipei)* **38**, 949 (2000).
- ⁸J. A. Rayne and B. S. Chandrasekhar, *Phys. Rev.* **122**, 1714 (1961).
- ⁹M. W. Guinan and D. N. Beshers, *J. Phys. Chem. Solids* **29**, 541 (1968).
- ¹⁰A. K. Singh, H. K. Mao, Jinfu Shu, and R. J. Hemley, *Phys. Rev. Lett.* **80**, 2157 (1998).
- ¹¹T. H. K. Barron and M. L. Klein, *Proc. Phys. Soc. London* **85**, 523 (1965).
- ¹²B. B. Karki, S. J. Clark, M. C. Warren, H. C. Hsueh, G. J. Ackland, and J. Crain, *J. Phys.: Condens. Matter* **9**, 375 (1997).
- ¹³L. Stixrude and R. E. Cohen, *Geophys. Res. Lett.* **22**, 125 (1995).
- ¹⁴M. Ross, D. A. Young, and R. Grover, *J. Geophys. Res.* **95**, 21713 (1990).
- ¹⁵J. M. Brown and R. G. McQueen, *Geophys. Res. Lett.* **7**, 533 (1980); *J. Geophys. Res.* **91**, 7485 (1986).